

The rise of spin-flip transitions in the anomalous Hall effect of FePt alloy

Hongbin Zhang, Frank Freimuth, Stefan Blügel, and Yuriy Mokrousov*
Institut für Festkörperforschung and Institute for Advanced Simulation,
Forschungszentrum Jülich and JARA, D-52425 Jülich, Germany

Ivo Souza
Department of Physics, University of California, Berkeley, CA 94720, USA
(Dated: September 7, 2018)

We carry out *ab initio* calculations which demonstrate the importance of spin-flip transitions for the intrinsic anomalous Hall conductivity of ordered FePt alloys. We show the such transitions get enhanced by large spin-orbit coupling of Pt atoms, becoming negligible when Pt is replaced by lighter isoelectronic Pd. We find that spin-flip transitions in FePt originate not only from conventional band anticrossings at the Fermi level, but also from transitions between well-separated pairs of bands with similar dispersions. We also predict a strong anisotropy in the anomalous Hall conductivity of FePt, which comes from spin-flip transitions entirely, and investigate the influence of disorder on it.

The intrinsic anomalous Hall effect (AHE) [1] and spin Hall effect (SHE) [2] in solids arise from the opposite anomalous velocities experienced by spin-up and spin-down electrons as they move through the spin-orbit-coupled bands under an applied electric field. In paramagnets, where the bands are normally spin-degenerate, these counter-propagating transverse currents result in a time-reversal (T) conserving pure spin current. In ferromagnets, where the bands are split by the exchange interaction, the same process generates a net T -odd charge current.

The above picture is intuitively appealing, and often leads to correct conclusions. However, it leaves out the fact that in the presence of spin-orbit coupling the spin projection along the quantization axis is not a good quantum number. This is a particularly subtle point regarding the SHE, as the proper definition of the spin current becomes problematic when spin is not a conserved quantity [3]. More generally, processes which do not conserve spin are known to play a role in phenomena such as spin relaxation [4] and magnetocrystalline anisotropy [5]. It is however usually assumed that such *spin-flip* processes can be safely ignored when studying transport. This viewpoint is supported by recent calculations of the intrinsic AHE [6] and extrinsic SHE [7].

In this work we use first-principles calculations to study the impact of spin-flip transitions on the intrinsic anomalous Hall conductivity (AHC) of FePt ordered alloys [8]. We find that their effect is considerable, as they account for about one fifth of the net AHC. More importantly, the calculations reveal a clear experimental signature of the spin-flip AHC: as the magnetization is rotated from the uniaxial direction to the basal plane, the spin-flip contribution changes sign, leading to a factor-of-two reduction in the net AHC, while the spin-conserving part is almost perfectly isotropic.

We identify two distinct mechanisms for the spin-flip transitions. The first involves spin-orbit-induced anticrossings at the intersections of up- and down-spin Fermi-

surface sheets (the locus of intersection forms loops in k -space, which we shall refer to as *hot loops*, in analogy with the *hot spots* that have been discussed in connection with spin-relaxation [4]). The second mechanism involves spin-orbit driven transitions between bands with similar dispersion which are split in energy across the Fermi level. We shall refer to them as *ladder* transitions. Both features occur at very low frequencies, of the order of the spin-orbit coupling strength.

Let us briefly review the formalism for calculating the intrinsic AHC from first-principles. For a ferromagnet with the orthorhombic crystal structure and magnetization \mathbf{M} along the \hat{z} ([001]) axis, the intrinsic anomalous Hall conductivity (AHC) $\sigma_z \equiv \sigma_{xy}$ is given by the k -space integral of the Berry curvature [1, 9]:

$$\sigma_z = \frac{e^2 \hbar}{4\pi^3} \text{Im} \int_{\text{BZ}} d\mathbf{k} \sum_{n,m}^{\text{o,e}} \frac{\langle \psi_{n\mathbf{k}} | v_x | \psi_{m\mathbf{k}} \rangle \langle \psi_{m\mathbf{k}} | v_y | \psi_{n\mathbf{k}} \rangle}{(\varepsilon_{m\mathbf{k}} - \varepsilon_{n\mathbf{k}})^2}. \quad (1)$$

In this expression $\psi_{n\mathbf{k}}$ and $\psi_{m\mathbf{k}}$ are respectively the occupied (o) and empty (e) spinor Bloch eigenstates of the crystal, v_x and v_y are components of the velocity operator \mathbf{v} , and the integral is over the Brillouin zone (BZ). When the direction of \mathbf{M} is changed from the \hat{z} -axis to the \hat{x} -axis ([100]), the $\sigma_x \equiv \sigma_{yz}$ component of the conductivity tensor should be calculated instead, by replacing $v_x \rightarrow v_y$ and $v_y \rightarrow v_z$ in Eq. (1).

The calculations were done using the approach of Ref. [10], whereby the linear-response expression (1) is rewritten in the basis of Wannier functions spanning the occupied and low-lying empty states. In this way the infinite sums over bands are replaced by sums over the small number of Wannier-interpolated bands. The Wannier functions were generated with WANNIER90 [11] using the same parameters as in Ref. [8], by post-processing first-principles calculations done using the Jülich DFT FLAPW code FLEUR [12] (see Ref. [13] for details). The unit cell contained two atoms in the $L1_0$ structure, with stacking along the [001]-direction and lattice constants

		Total	$\sigma^{\uparrow\uparrow}$	$\sigma^{\uparrow\downarrow}$	$\Delta\sigma^{\uparrow\uparrow}$	$\Delta\sigma^{\uparrow\downarrow}$
FePt	[001]	818.1	576.6	133.4	-8.5	317.3
	[100]	409.5	585.1	-183.9		
FePd	[001]	135.1	108.4	28.4	-88.5	-33.6
	[100]	275.9	196.9	62.0		

TABLE I: Values of the AHC for [001] (σ_z) and [100] (σ_x) directions of magnetization \mathbf{M} in FePt and FePd. $\Delta\sigma^{\uparrow(\downarrow)}$ is defined as the difference between no-flip (flip) parts of σ_z and σ_x . All values are in S/cm.

$a = 5.14$ a.u. and $c = 7.15$ a.u. [14].

The spin-orbit term in the Hamiltonian has the form

$$\xi \mathbf{L} \cdot \mathbf{S} = \xi L_{\hat{n}} S_{\hat{n}} + \frac{\xi}{2} (L_{\hat{n}}^+ S_{\hat{n}}^- + L_{\hat{n}}^- S_{\hat{n}}^+), \quad (2)$$

where ξ is the spin-orbit coupling strength and \hat{n} is the magnetization direction, which is taken as the spin-quantization axis. The first term on the r.h.s. of Eq. (2), which we will denote as $LS^{\uparrow\uparrow}$, preserves the spin of a pure-spin state $\psi_{n\mathbf{k}}$, while the second term, $LS^{\uparrow\downarrow}$, flips it. The spin-flip ($\sigma^{\uparrow\downarrow}$) and spin-conserving ($\sigma^{\uparrow\uparrow}$) parts of the AHC σ are calculated from Eq. (1) after selectively turning off the $LS^{\uparrow\downarrow}$ or $LS^{\uparrow\uparrow}$ parts of the SOI Hamiltonian (2). We find that to a very good approximation they are additive, i.e., $\sigma \approx \sigma^{\uparrow\uparrow} + \sigma^{\uparrow\downarrow}$.

The importance of spin-flip transitions for the AHC of FePt can be seen by analyzing its dependence on the magnetization direction (see Table 1). If only the spin-conserving term in Eq. (2) is kept, the resulting AHC $\sigma^{\uparrow\uparrow}$ changes by less than 2% from an average value of about 580 S/cm as \mathbf{M} is tilted from the \hat{z} -axis to the \hat{x} -axis. When the spin-flip term is also included in the calculation, the AHC becomes highly anisotropic, decreasing by a factor of two from [001] to [100]. Keeping only the spin-flip part of the SOI reveals that it is indeed responsible for the large anisotropy, as the resulting AHC changes by more than 300 S/cm, from a positive value along [001] to a negative value along [100]. Such large AHC anisotropy can occur in uniaxial crystals, and was previously found in hcp Co [15], however, as opposed to FePt, in hcp Co the anisotropy is caused for the most part by spin-conserving transitions.

Such a large spin-flip contribution in FePt is rather unexpected, in view of the fact that in a perturbative expansion in powers of ξ only the spin-conserving part of the SOI Hamiltonian (2) contributes to Eq. (1), with spin-flip appearing only at second order [16]. It should however be kept in mind that because Pt is a heavy atom, the SOI cannot be treated as a small perturbation in FePt. Moreover, the AHC is very sensitive to near-degeneracies across the Fermi level [9], and therefore the above analysis of Ref. [16], which is based on non-degenerate perturbation theory, may not apply.

The AHC can be resolved in energy by defining a cu-

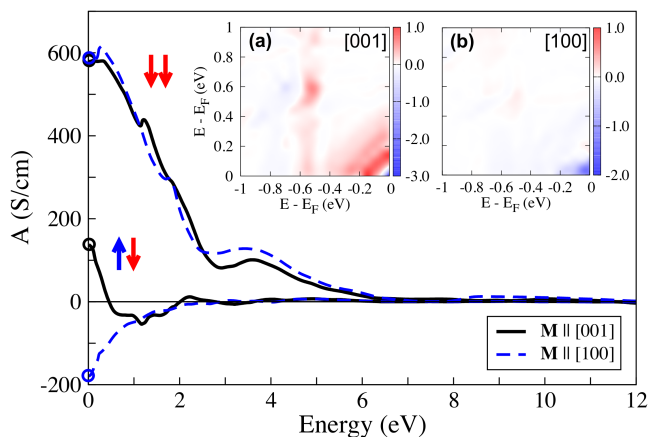


FIG. 1: (color online) Spin-flip ($\uparrow\downarrow$) and spin-conserving ($\uparrow\uparrow$) cumulative contribution to the AHC from the spectrum above energy ω , $A(\omega)$. Inset presents the energy-energy density of contributions to the flip-AHC, $\Sigma(\varepsilon_1, \varepsilon_2)$, for \mathbf{M} along (a) [001] and (b) [100]-axes (in 10^5 a.u./eV²). Open circles indicate the values of AHC from Table 1.

mulative AHC $A(\omega)$, which accumulates all transitions in Eq. (1) for which $\varepsilon_{m\mathbf{k}} - \varepsilon_{n\mathbf{k}} > \omega$ [15]. In the limit $\omega \rightarrow 0$ all interband transitions are accounted for, and $A(\omega = 0)$ equals the full AHC. The spin-conserving and spin-flip contributions to the cumulative AHC are plotted in Fig. 1 in the range $0 \leq \omega \leq 12$ eV, for both $\mathbf{M} \parallel \hat{z}$ and $\mathbf{M} \parallel \hat{x}$. While $A^{\uparrow\uparrow}(\omega)$ remains largely isotropic over the entire energy range and decays rather slowly with ω up to 4–5 eV in energy, the $A^{\uparrow\downarrow}(\omega)$ contribution picks up only for ω below 1 eV and immediately becomes strongly anisotropic with decreasing energy, displaying a characteristic bifurcation shape [15]. Thus, the anisotropy in the AHC arises from spin-flip transitions in the 0.5 eV energy window around E_F .

To get a further insight into which kind of transitions is responsible for $A^{\uparrow\downarrow}(\omega)$, we calculate the density of contributions to the AHC given by Eq. (1), $\Sigma(\varepsilon_1, \varepsilon_2)$, from the states with energies $\varepsilon_1 < E_F$ and $\varepsilon_2 > E_F$. The overall integral $\iint \Sigma(\varepsilon_1, \varepsilon_2) d\varepsilon_1 d\varepsilon_2$ provides the value of $\sigma^{\uparrow\downarrow}$, while assuming the constraint $\varepsilon_2 - \varepsilon_1 > \omega$, this integral gives the value of $A^{\uparrow\downarrow}(\omega)$. Density Σ can be used in combination with the cumulative AHC to obtain more information on the energy structure of the Berry curvature and the anomalous Hall conductivity.

The calculated density Σ for $\mathbf{M} \parallel \hat{z}$ and $\mathbf{M} \parallel \hat{x}$ is presented in Fig. 1(a) and (b), respectively. In these plots we can clearly see the contributions from the band anti-crossings of \uparrow - and \downarrow -bands along the hot loops in the BZ. They are given by blue dots around the origin $\varepsilon_1 = \varepsilon_2 = 0$ and provide a negative contribution to the AHC for both magnetization directions. While for $\mathbf{M} \parallel \hat{x}$ the hot loops contribution dominates, for $\mathbf{M} \parallel \hat{z}$ a competing positive contribution to the AHC can be clearly seen in Fig. 1(a).

	Fe ^{tot}	Fe ^{↑↑}	Fe ^{↑↓}	Pt ^{tot}	Pt ^{↑↑}	Pt ^{↑↓}
[001]	-13.7	17.9	-26.8	848.0	541.0	282.3
[100]	210.0	253.6	-37.5	65.0	425.7	-360.6

TABLE II: Atomically resolved values of the AHC for [001] and [100] directions of magnetization \mathbf{M} in FePt, decomposed into $\uparrow\uparrow$ - and $\uparrow\downarrow$ -contributions. All values are in S/cm.

It is given by series of stripes $\varepsilon_2 - \varepsilon_1 \approx \text{const.}$ in the vicinity of the Fermi energy. By analyzing the band structure we find that these transitions come from pairs of bands of different orbital character with similar dispersion around E_F (see inset in Fig. 2). Such ladder transitions, induced by SOI, provide a different source of the AHC as they do not require a band crossing at the Fermi energy, and occur over large regions in energy and k -space. In case of FePt with $\mathbf{M} \parallel \hat{z}$ their contribution is so large that it wins over the hot-loops part and determines the sign and magnitude of the flip-AHC.

The spin-flip contribution to the AHC in FePt originates from heavy Pt atoms. To demonstrate this we decompose the spin-orbit part of the Hamiltonian in FePt in real space as

$$H^{\text{SO}} = \xi_{\text{Fe}} \mathbf{L}^{\text{Fe}} \cdot \mathbf{S} + \xi_{\text{Pt}} \mathbf{L}^{\text{Pt}} \cdot \mathbf{S}, \quad (3)$$

where \mathbf{L}^μ is the orbital angular momentum operator associated with atom μ and ξ_μ is the averaged over valence d -orbitals spin-orbit coupling strength. For an Fe atom in FePt the SOI strength ξ_{Fe}^0 amounts to 0.06 eV, with corresponding value of $\xi_{\text{Pt}}^0 = 0.54$ eV.

By using together representations of SOI according to (2) and (3), we perform a $\uparrow\uparrow$ - and $\uparrow\downarrow$ -decomposition of the AHC coming separately from Fe and Pt atoms, presenting results in Table 2. It can be seen, that when we consider contribution to the AHC from only Fe atoms by setting ξ_{Pt} in (3) to zero, for $\mathbf{M} \parallel \hat{z}$ both $\uparrow\uparrow$ - and $\uparrow\downarrow$ -AHC are very small, and while the Fe-driven $\sigma^{\uparrow\downarrow}$ remains also very small for the in-plane magnetization, $\sigma^{\uparrow\uparrow}$ dominates in this case. On the other hand, by analyzing the Pt-originated AHC ($\xi_{\text{Fe}} = 0$), we observe that the spin-flip part is very large for both magnetization directions. For $\mathbf{M} \parallel \hat{z}$ the sum of Pt $\sigma^{\uparrow\uparrow}$ and $\sigma^{\uparrow\downarrow}$ results in a large total AHC manifesting that for this magnetization direction the AHE is driven by Pt atoms. For $\mathbf{M} \parallel \hat{x}$, the Pt $\sigma^{\uparrow\downarrow}$ is of the same magnitude but of opposite sign to its $\uparrow\uparrow$ -counterpart, and both conductivities almost cancel – in this case the Hall current in FePt is mainly of Fe origin.

When decreasing the SOI strength in FePt by substituting Pt atoms with Pd atoms in FePd alloy, we see an essential decrease in the values of spin-flip AHC, as compared to the total AHC for both magnetization directions (Table 1), which is in correspondence to the perturbation theory arguments [17]. For FePd, the AHC anisotropy is mainly driven by $\Delta\sigma^{\uparrow\uparrow}$, which is of the same sign and somewhat larger magnitude than $\Delta\sigma^{\uparrow\downarrow}$ in FePt, while

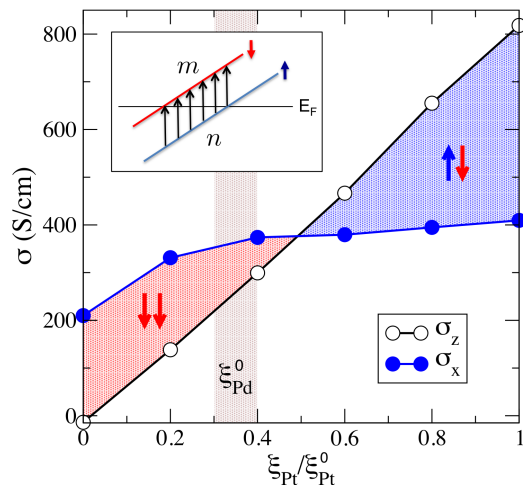


FIG. 2: (color online) Dependence of σ_z (open circles) and σ_x (filled circles) in FePt alloy on the SOI strength inside the Pt atoms ξ_{Pt} with respect to its unscaled value ξ_{Pt}^0 . Arrows indicate the spin-flip ($\uparrow\downarrow$) or spin-conserving ($\uparrow\uparrow$) nature of the AHC anisotropy. Inset shows transitions in Eq. (1) leading to the ladder contribution to the flip-AHC.

the total AHC anisotropy is opposite in sign to that in FePt, c.f. Table 1. In the following we make sure that such differences between the AHC of FePt and FePd are indeed caused by different SOI strength and not by other details of the electronic structure, such as Stoner parameters, spread of d -functions etc.

Without affecting SOI on Fe atoms, we scale down the ξ_{Pt}^0 constant in FePt, Eq. (3), and perform self-consistent calculations of the σ_z and σ_x conductivities with the new corresponding SOI strength, ξ_{Pt} . The results of these calculations are presented in Fig. 2 as a function of $\xi_{\text{Pt}}/\xi_{\text{Pt}}^0$. In this figure we observe, that while the decay of σ_z is almost perfectly linear, the σ_x conductivity stays almost constant until the regime of ξ_{Pt} corresponding to the SOI strength of Pd atoms in FePd alloy $\xi_{\text{Pd}}^0 = 0.19$ eV (indicated with shaded area in Fig. 2). This can be explained by the fact that for $\mathbf{M} \parallel \hat{x}$ the AHC comes from Fe atoms and thus it is not sensitive to ξ_{Pt} , however, the AHC for $\mathbf{M} \parallel \hat{z}$ is mostly Pt-originated (see Table 2), with ξ_{Pt} serving as effective SOI strength of the system in this case.

At the value of $\xi_{\text{Pt}} \approx \xi_{\text{Pt}}^0/2$, σ_x starts dominating over σ_z , with values of AHC and its anisotropy qualitatively close to those in FePd, when ξ_{Pt} reaches ξ_{Pd}^0 . We conclude that the difference in value and sign of the AHE anisotropy between FePt and FePd alloys can indeed be attributed solely to the SOI strength of Pt and Pd atoms, and the crossover between $\downarrow\downarrow$ - and $\uparrow\downarrow$ -contributions with the SOI strength thus explains different sign of the AHC anisotropy in FePt and FePd, Fig. 2. Therefore, we suggest to use Pd-doped FePt in order to tune the effective

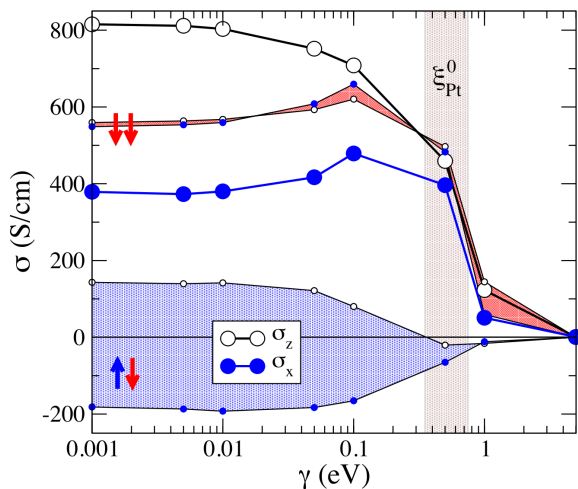


FIG. 3: (color online) Dependence of the σ_z (open circles) and σ_x (filled circles) in FePt on quasiparticle damping rate γ , calculated within the Kubo-Štreda formula. The area between $\uparrow\uparrow$ - and $\uparrow\downarrow$ -AHC for two different magnetization directions is shaded in red and blue, respectively.

SOI strength as well as spin-character and sign of the AHE anisotropy in these alloys.

Finally, we investigate the influence of disorder on the AHC and its anisotropy in FePt. For this purpose, using the tight-binding formulation in terms of the Wannier functions, we employ the Kubo-Štreda formula [18] for the AHC in the "constant γ approximation", assuming that the quasiparticle damping rate γ is independent of the orbital [19]. The validity of this approximation for investigations of SHE and AHE in transition metals has been demonstrated [6, 19]. The results of our calculations for σ_z (open circles) and σ_x (filled circles) as a function of disorder characterized by quasiparticle lifetime $1/\gamma$ are presented in Fig. 3, and allow for a simple explanation in terms of energy scales discussed previously.

Upon increasing disorder, isotropic $\sigma^{\uparrow\uparrow}$ (red shaded area) stays practically constant until γ of 0.1 eV, then decreases upon further increasing γ and disappears at γ of 4–5 eV – a value, which characterizes the decay of the $\uparrow\uparrow$ -cumulative AHC with energy, c.f. Fig. 2, and roughly corresponds to the characteristic band width in FePt. The $\uparrow\downarrow$ -AHC (blue shaded area), on the other hand, decays much faster, and disappears at the value of γ around 0.5 eV corresponding to the width of $A^{\uparrow\downarrow}$ in Fig. 2. This value can be traced back to the Pt SOI strength ξ_{Pt}^0 (grey shaded area in Fig. 3), which emphasizes Pt origin of spin-flip contribution to the AHC. Upon γ reaching ξ_{Pt}^0 the interband coherence necessary for a build-up of $\uparrow\downarrow$ -AHC is destroyed and $\sigma^{\uparrow\downarrow}$ goes to zero. The relative robustness of $\sigma^{\uparrow\uparrow}$ with respect to γ , as compared to $\sigma^{\uparrow\downarrow}$, underlines the fact that the spin-flip transitions, living on

a different energy scale, are much more sensitive to the degree of crystallinity, and are affected stronger by disorder. Overall, after adding up $\uparrow\uparrow$ - and $\uparrow\downarrow$ -AHC we observe that while the total σ_z (large open circles) monotonously decreases with γ and drops significantly upon γ reaching ξ_{Pt}^0 , σ_x (large filled circles) stays relatively constant in this range of disorder, with both conductivities vanishing at γ of several eV. This qualitatively different behavior of σ_z and σ_x upon increasing disorder brings us to a conclusion that up to a certain extent, the degree of disorder in FePt serves as the SOI strength ξ_{Pt} , c.f. Fig. 2, in accord to experimental findings [20].

To conclude, we predict a strong anisotropy of the intrinsic AHC in FePt and FePd alloys. We show, that while in FePt the AHC anisotropy arises purely due to Pt-driven spin-flip transitions in a small energy window around E_F , upon decreasing the SOI strength on Pt atoms, the sign of this anisotropy and its nature can be changed in Pd-containing alloys. We also demonstrate that in FePt the AHE comes from different types of atoms depending on the direction of the magnetization and that the degree of disorder in the samples of FePt can serve as an effective SOI strength of Pt atoms.

We acknowledge discussions with M. Ležaić, Ph. Mavropoulos and K. M. Seemann. We also thank HGF-YIG Programme VH-NG-513 for funding and supercomputers JUROPA and JUGENE for computational time.

* corresp. author: y.mokrousov@fz-juelich.de

- [1] N. Nagaosa *et al.*, Rev. Mod. Phys. **82**, 1539 (2009)
- [2] J.E. Hirsch, Phys. Rev. Lett. **83**, 1834 (1999)
- [3] J. Shi *et al.*, Phys. Rev. Lett. **96**, 76604 (2006)
- [4] I. Žutić *et al.*, Rev. Mod. Phys. **76**, 323 (2004)
- [5] C. Andersson *et al.*, Phys. Rev. Lett. **99**, 177207 (2007)
- [6] T. Naito *et al.*, Phys. Rev. B **81**, 195111 (2010)
- [7] M. Gradhand *et al.*, Phys. Rev. Lett. **104**, 186403 (2010)
- [8] K. Seemann *et al.*, Phys. Rev. Lett. **104**, 076402 (2010)
- [9] Y. Yao *et al.*, Phys. Rev. Lett. **92**, 037204 (2004)
- [10] X. Wang *et al.*, Phys. Rev. B **74**, 195118 (2006)
- [11] A. A. Mostofi *et al.*, Comput. Phys. Commun. **178**, 685 (2008)
- [12] www.flapw.de
- [13] F. Freimuth *et al.*, Phys. Rev. B **78**, 035120 (2008)
- [14] For $L1_0$ FePd we used the values of c and a of 7.15 a.u. and 5.12 a.u., respectively.
- [15] E. Roman *et al.*, Phys. Rev. Lett. **103**, 097203 (2009)
- [16] B. R. Cooper, Phys. Rev. **139**, A1504 (1965)
- [17] In $L1_0$ FeNi alloy with ξ_{Ni}^0 of 0.05 eV our calculated values of σ_z and σ_x constitute 165.7 and 284.8 S/cm, respectively, with $\uparrow\downarrow$ -contribution of about 30 S/cm. Corresponding spin-flip anisotropy $\Delta\sigma^{\uparrow\downarrow}$ is only 0.9 S/cm.
- [18] P. Štreda, J. Phys. C **15**, L717 (1982)
- [19] T. Tanaka *et al.*, Phys. Rev. B **77**, 165117 (2008)
- [20] M. Chen *et al.*, arXiv: 1004.0548v3 (2010)